CSIAM Trans. Appl. Math.
doi: 10.4208/csiam-am.SO-2025-0014

Vol. **x**, No. x, pp. 1-27
xx 2025

# Bifurcation and Crossover Processes in the Dynamics of a Marburg Haemorrhagic Fever Model

EF. Doungmo Goufo[1,*] and I. Tchangou Toudjeu[2]

[1] *Mathematical Sciences, University of South Africa, Florida 0003, South Africa.*
[2] *Department of Electrical Engineering, Tshwane University of Technology, Pretoria 183, South Africa.*

Received 14 February 2025; Accepted 16 July 2025

**Abstract.** Just like Ebola disease, the Marburg virus disease (MVD) remains a constant threat to people's live, not only in Africa, but also in the other parts of the globe. Recorded past outbreaks occurred in Europe, America and of course Africa, especially in places where inhabitants come into contact with wild animal products or live alongside wild animals such as apes, monkeys and fruit bats on a daily basis. Therefore, studying the dynamics of the Marburg virus and making some epidemiological assessments remain relevant and important in preventing future outbreaks. In this paper, we analyze a Marburg epidemic model in which the transmission is nonlinear. The well-posedness result is established as well as conditions for boundedness and dissipativity results. Then, we intensively analyze the stability of the Marburg model's equilibria. The bifurcation dynamics indicate the existence of both transcritical (exchange of stability between the endemic equilibrium (EE) point and the disease free equilibrium (DFE)) and backward bifurcation where the classical epidemiological condition for the MVD to die out ($\mathcal{R}_0<1$) is not sufficient anymore, but remains necessary. Lastly, some numerical simulations show convergence of the trajectories to both the EE and the DFE. Some adequate preventive measures are provided.

**AMS subject classifications**: 26A33, 37M05, 65P30, 65P40

**Key words**: Marburg hemorrhagic fever model, numerical solvability, filovirus, nonlinear incidence, bifurcation, crossover, stability.

## 1 Introduction

The Marburg virus (MARV) is seen as an extremely pathogenic virus thats causes a severe disease leading to mortality rates fluctuating between 20% and 90%. For the genetic side,

*Corresponding author. *Email addresses:* franckemile2006@yahoo.ca (EF. Doungmo Goufo), itchangou@gmail.com (I. Tchangou Toudjeu)

 

the MARV is characterized by a genome packaged into a unique filamentous virion with length varying between 790 and 970 nm and width of 80 nm [15, 32]. It was first identified in 1967 in the towns of Marburg and Frankfurt (Germany) and Belgrade (Serbia formerly known as Yugoslavia), during a series of outbreaks in which number of laboratory workers were exposed to blood and tissues of infected grivet monkeys, a kind of African green monkeys imported from Uganda. The outbreaks saw the deaths of seven people out of the thirty-one that became infected [33]. It chronology and early evolution is depicted in Fig. 1. The world experienced many MARV outbreaks and most of them remained sporadic if not occasional. In human population, the disease caused by the MARV is known as the Marburg virus disease. Just like Ebola virus, the Marburg virus also belongs to the family of Filoviridae which regroups number of genera such as Thamnovirus, Cuevavirus and of course Ebolavirus and Marburgvirus. The virus causing the MVD belongs to the filovirus family, which is also part of Marburgvirus genera. Viruses from the filovirus family can provoke hemorrhagic fever and death in both human and non-human populations, such as primates (as depicted in Figs. 2-3). It appears to be deadly with the severity amplified by the lack of adequate infrastructures and amenities able to timely to detect, diagnose, prevent and treat the disease [22, 23, 25, 32]. The MVD usually starts by a severe sore throat, headache and fever followed by maculopapular rash all over the torso down to the limbs and a red exanthem appearing on both the front part and back part of the palate. The patient during the first five days of the symptoms, can suffer from body pain together with nausea, diarrhea and we can see the intensification of hemorrhagic fever's symptoms like mucosal bleeding, bleeding from venipuncture sites and presence of blood in the faeces and vomits. The patient becomes lethargic and he gets dehydrated due to watery diarrhea and vomiting. Internal hemorrhage, organ failure together with the dysregulated immune response to the virus


Figure 1: The Marburg virus disease: origin, evolution and parties involved [30].

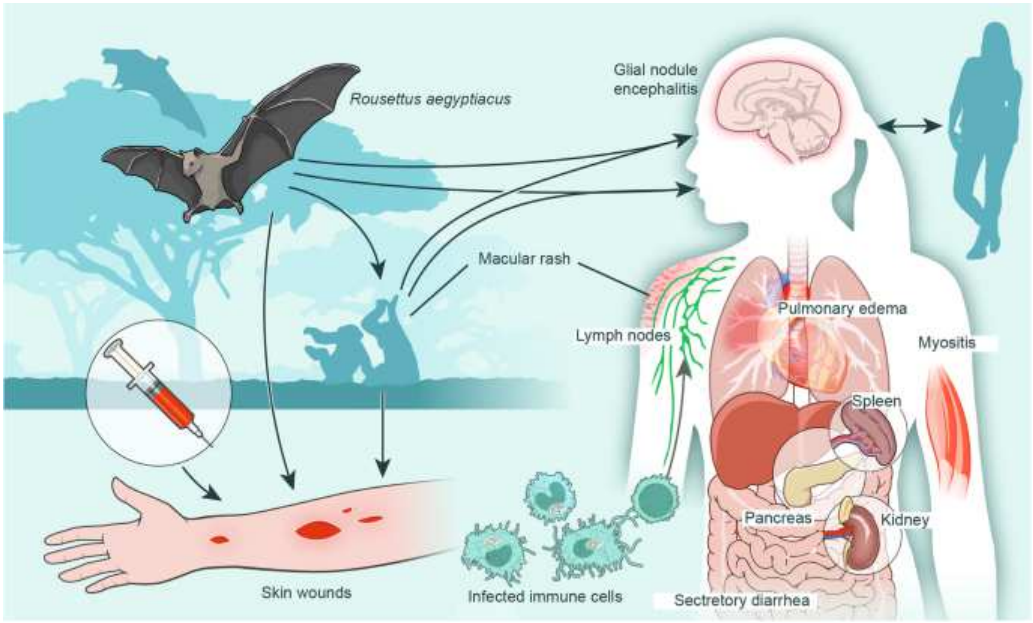


Figure 2: Transmission dynamics of the Marburg virus as it spreads in the human population [32].

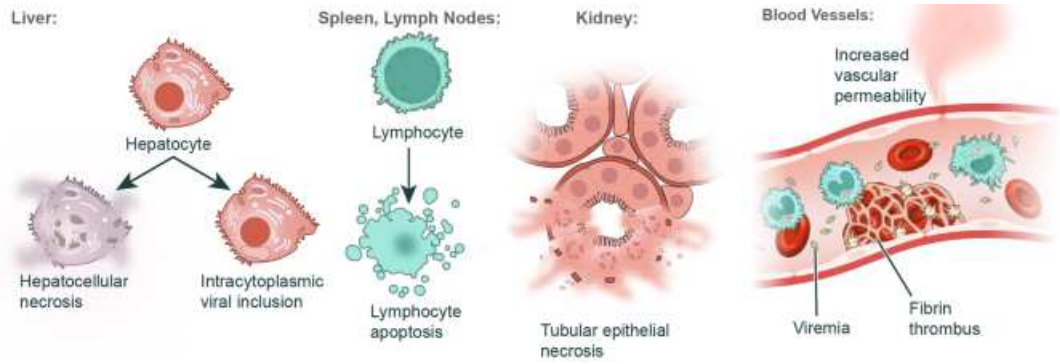


Figure 3: Possible tissue damages caused by Marburg virus as it spreads in the human body [32].

may lead to death. However, not every patient dies and those who survive usually have mild late stage symptoms of the disease. However, during and after recovery, they may suffer from symptoms of arthritis, conjunctivitis, myalgia, and psychosis [30].

The MARV is highly transmissible to humans via exposure to some fruit bats and human to human through body fluids, unprotected sex or broken skin. Many patients, depending on their level of natural or induced immunity, may develop violent haemorrhagic effects between five and seven days. The patients who are fatally affected usually present some kind of bleeding, from different parts of the body. The blood found in vomitus sometimes goes with bleeding from the nose and gums, whereas the blood found in faeces goes with bleeding from orifices like vagina. Another manifestation of the in-

fection is the sudden bleeding occurring during intravenous access for the purpose of blood sampling (phlebotomy) and which can be can be particularly laborious for the patient [36]. The patient's central nervous system is highly involved in the development of the disease and the consequences are various: Grumpiness, confusion, violence and aggression.

The world has so far experienced number of outbreaks of Marburg virus with the most recent one that happened, from 25 July to 16 September 2021 in the district of Gueckedou (Guinea). Fortunately only one person become infected with the disease and died, with no other known cases reported [35, 36]. However, there have been, in the past, other outbreaks in African countries such Angola, Zimbabwe, South Africa, Kenya, Democratic Republic of the Congo and Uganda [12,17,37]. These recorded Marburg hemorrhagic fever outbreaks have fatally affected fewer people compared to Ebola virus outbreaks. Most of affected people were adults, excepts the Angola 2005's outbreak in which a high proportion of children were affected and which killed 227 people [16, 25, 27, 35]. The MVD is generally recognized when there are outbreaks. A successful control of these different outbreaks requires measures such as Risk communication and community engagement (RCCE). Making people and community to become aware of the risk factors linked to Marburg infection and protective directives that individuals can consider to limit human exposure to the MARV are substantial in reducing infections and potential deaths.

The recent Marburg virus outbreak occurs in the Republic of Rwanda which has confirmed more than seventy cases in the country, and primarily based in the capital city Kigali, where some deaths were recorded. This is the country's first Marburg outbreak. Before that, a series of cases of infections were reports in various parts of Africa, particularly in countries like Guinea and Tanzania. The World Health Organization (WHO) and other health agencies have been closely monitoring and responding to these outbreaks, providing support for containment measures and treatment efforts [4].

Lately in January 2025, in the Democratic Republic of the Congo, a new, unrecognized disease presenting symptoms like the Ebola ones surfaced, leading to over 50 deaths in about five weeks . Early inquiries traced the source of the outbreak to Boloko village, after bat meat was consumed. Laboratory tests for common hemorrhagic fevers, including Marburg disease, returned negative. Hence, up to now, the exact cause remains under investigation [38].

In the following section, we consider and analyze a generalized mathematical model describing the Marburg disease dynamics in a particular region. We also studies different stability conditions related to this specific model.

## 2 Model formulation

We consider here a region where the total population at the time $t$ is denoted by $N(t)$, with the initial population $N(0) = N_0$. We divide the population $N(t)$ into four sub-

classes: $S(t), I(t), R(t)$ and $U(t)$ respectively the compartments of susceptible individuals, infected individuals, recovered individuals and immunized individuals. In fact, $S(t)$ comprises individuals considered to be susceptible to get MARV, while $I(t)$ comprises individuals infected with MARV. Those individuals who recover from MARV are comprised in $R(t)$ and lastly we believe that some individuals become immunized after being infected and recovered from MARV and they are comprised in the compartment $U(t)$. All recruitments are assumed to be happening at the rate constant $\Lambda$, into the $S(t)$ compartment of susceptible individuals. We also assume that infected individuals become automatically infectious.

A fraction of the population $N(t)$ is assumed to be dying at a rate constant $\theta$ from the causes non related to MVD, making the quantity $1/\theta$ the average lifetime. Furthermore, people are assumed to be killed by the MARV at a rate constant $d$. The successful MARV transmission is assumed to be nonlinear, indicating the kind of contacts between people in the population and the infectious, and given by the incidence $\beta S\eta(I)$ where $\beta$ represents a rate constant. The nonlinear character of the dynamics is symbolized by function $\eta$ with $\eta(0)=0$ and $\eta(I)>0$ for $0<I\leq N_0$. The function $\eta$ belongs at least to the space $C^3(0,N_0]$.

We also assume that MARV infectious individuals, thanks to some biological protective systems or efficient treatments, suddenly recover from the MVD at a rate constant $\sigma$, allowing them to enter the compartment of recovered individuals. Among those who recover, we believe that a fraction of them, $\nu R$ with $\nu\leq 1$ become immunized due to the treatments received, making the remaining fraction $(1-\nu)R$ susceptible again to catch the MARV a rate constant $\zeta$. The above description is summarized in the transfer diagram depicted in Fig. 4 and mathematically expressed by the following system:

$$\begin{cases} {}^cD_t^\gamma S=\Lambda-[\beta\eta(I)+\theta]S+(1-\nu)\zeta R,\\ {}^cD_t^\gamma I=\beta S\eta(I)-(\theta+\sigma+d)I,\\ {}^cD_t^\gamma R=\sigma I-[(\theta+\nu)+(1-\nu)\zeta]R,\\ {}^cD_t^\gamma U=\nu R-\theta U \end{cases} \tag{2.1}$$

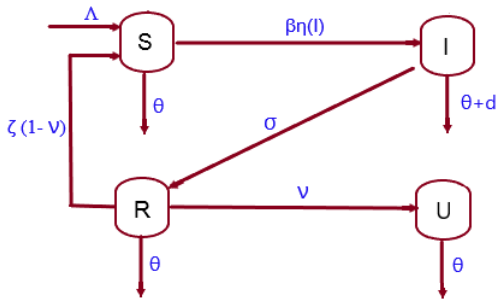


Figure 4: Flow diagram of the Marburg model.

with the initial conditions reading as

$$S(0)=S_0,\quad I(0)=I_0,\quad R(0)=R_0,\quad U(0)=U_0. \tag{2.2}$$

Here ${}^cD_t^\gamma$ is the Caputo derivative mathematically defined as

$${}^cD_t^\gamma u(t)=\frac{1}{\Gamma(1-\gamma)}\int_0^t (t-\tau)^{-\gamma}\frac{du}{d\xi}(\xi)d\xi. \tag{2.3}$$

# 3 Mathematical analysis

The main aim of this section is to first analyze the well-posed of the system (2.1)-(2.2). After that we investigate the existence results for the system's equilibrium points. Before that, let us recall that using fractional differential equations for modelling diseases gives us a larger degree od liberty than traditional differential equations do. Hence, there has been growing interests among the scientific community about applying fractional operators to the domain of modelling in mathematical epidemiology because disease dynamics and related phenomena in different fields, like sciences, engineering, and technology, have proven to be described successfully by the systems using fractional-order operations and such descriptions appear to be better compared to the classical ones. As an example, modelling in mathematical epidemiology where we use the concept of a fractional Laplacian operator (theory of Lévy flights) is a typical application of a better described process based on fractional derivatives [6,10,29].

## 3.1 Positivity and boundedness results

Firstly, we prove that, for any $t\geq 0$, the solutions of model (2.1)-(2.2) with nonnegative initial conditions remain nonnegative. Moreover, we show that they are bounded. Consider the space

$$R_+^4=\{(S,I,R,U)\in R^4 : S\geq 0, I\geq 0, R\geq 0, U\geq 0\}.$$

We can refer to the fundamental theory of ordinary differential equations (ODEs) to state that there exists locally a unique solution $\mathfrak{S}=(S,I,R,U)$ for the Cauchy problem (2.1)-(2.2). Hence, we have the following results.

**Proposition 3.1.** *Let* $(S,I,R,U)$ *be a solution of* (2.1)-(2.2) *on* $[t_0,+\infty), t_0\in\mathbb{R}$. *If the initial condition* (2.2) *is non-negative, then the corresponding solution* $\mathfrak{S}$ *of the Marburg model* (2.1) *is non-negative for all* $t\in(t_0,t_1), t_1>0$.

*Proof.* Let us put $X_1=S, X_2=I, X_3=R$ and $X_4=U$. Assume that there is an instant $t$ at which a $X_j(t)$ vanishes for any $j=1,2,3,4$. Put

$$\tilde{t}=\inf\{t\in(t_0,t_1) : X_j(t)=0, j=1,2,3,4\}.$$

Then, for any $j=1,2,3,4$,

$$\begin{cases} X_j(t)>0, & t\in(t_0,\tilde{t}),\\ X_j(\tilde{t})=0. \end{cases}$$

Hence, using (2.1), the differential equation for the solution $X_j$ can take the form

$${}^cD_t^{\gamma}X_j=-X_jE(X)+\tilde{E}(X),$$

where $\tilde{E}(X)$ is a non-negative function. This yields

$$\begin{cases} {}^cD_t^{\gamma}X_j(t)\geq -X_jE(X), & t\in[t_0,\tilde{t}],\\ X_j(t)>0, & t\in[t_0,\tilde{t}], \end{cases}$$

which contradicts the fact that $X_j(\tilde{t})=0$ and the proof is complete. □

This results also proves that, with respect to model (2.1), the nonnegative orthant

$$R^4_+=\{(S,I,R,U)\in R^4 : S\geq 0, I\geq 0, R\geq 0, U\geq 0\}$$

is positively invariant. We can therefore state the following boundedness and compactness results.

**Proposition 3.2.** *The solutions of the system* (2.1) *are uniformly bounded in the compact subset*

$$\Psi_{\varepsilon}=\left\{(S;I;R;U)\in R^4_+, N(t)\leq \frac{\Lambda}{\theta}+\varepsilon\right\}. \tag{3.1}$$

*Thus, the subset $\Psi_{\varepsilon}$ is a positively-invariant set for the system* (2.1) *with non-negative initial conditions in $R^4_+$ and which is absorbing for $\varepsilon>0$. Moreover, we have the invariance property:*

$$\textit{If } N(0)\leq\frac{\Lambda}{\theta}, \textit{ then } N(t)\leq\frac{\Lambda}{\theta} \textit{ for all } t\geq 0, \textit{ and } \lim_{t\to+\infty}N(t)\leq\frac{\Lambda}{\theta}.$$

*Proof.* From the system (2.1), we get $N=S+I+R+U$ by summing all the equations, and

$${}^cD_t^{\gamma}N(t)=\Lambda-\theta N(t)-dI(t).$$

This leads to ${}^cD_t^{\gamma}N(t)\leq\Lambda-\theta N(t)$. The result follows as we use a method similar to that of the proof of the Proposition 3.1 above. □

### 3.2 Existence results and stability analysis

Let the system be

$$\begin{cases} {}^cD_t^{\gamma}S=\Lambda-\beta S\eta(I)+(1-\nu)\zeta R-\theta S,\\ {}^cD_t^{\gamma}I=\beta S\eta(I)-(\theta+\sigma+d)I,\\ {}^cD_t^{\gamma}R=\sigma I-(\theta+\nu)R-(1-\nu)\zeta R, \end{cases} \tag{3.2}$$

and

$$ {}^{c}D_{t}^{\gamma}N=\Lambda-\theta N-dI. \tag{3.3}$$

Solving the system

$$\begin{cases} 0=\Lambda-\beta S\eta(I)+(1-\nu)\zeta R-\theta S, \\ 0=\beta S\eta(I)-(\theta+\sigma+d)I, \\ 0=\sigma I-(\theta+\nu)R-(1-\nu)\zeta R, \\ 0=\Lambda-\theta N-dI, \end{cases} \tag{3.4}$$

we get the equilibria

$$X_o=\left(\frac{\Lambda}{\theta},0,0,\frac{\Lambda}{\theta}\right), \quad X_*=(S_*,I_*,R_*,N_*),$$

where

$$S_*=\frac{(\theta+\sigma+d)I_*}{\beta\eta(I_*)}, \quad R_*=\frac{\sigma I_*}{\theta+\nu+(1-\nu)\zeta}, \quad N_*=\frac{\Lambda-dI_*}{\theta},$$

and where $I_*$ verifies

$$\frac{\eta(I)}{I}\left[1-\left(\frac{(\theta+\sigma+d)\big(\theta+\nu+(1-\nu)\zeta\big)-(1-\nu)\zeta\sigma}{\Lambda\big(\theta+\nu+(1-\nu)\zeta\big)}\right)I\right]=\frac{\theta(\theta+\sigma+d)}{\Lambda\beta}. \tag{3.5}$$

### 3.2.1 The disease-free equilibrium (DFE)

We can study the stability of the DFE $X_o$ for the system (3.2)-(3.3), by analyzing the eigenvalues of the Jacobian matrix. Hence, the Jacobian matrix evaluated at the disease-free equilibrium $X_o$, using the linearized system (3.2)-(3.3) reads as

$$J(X_o)=Df(X_o)=\begin{pmatrix} -\theta & -\beta\frac{\Lambda}{\theta}\eta'(0) & (1-\nu)\zeta & 0 \\ 0 & \beta\frac{\Lambda}{\theta}\eta'(0)-(\theta+\sigma+d) & 0 & 0 \\ 0 & \sigma & -(\theta+\nu)-(1-\nu)\zeta & 0 \\ 0 & -d & 0 & -\theta \end{pmatrix}. \tag{3.6}$$

This allows us to state the following proposition.

**Proposition 3.3.** *Considering the definition of nonlinear incidence $\eta$ taken from the space $C^3(0,N_0]$, and assuming that the following condition holds:*

$$\frac{\beta\Lambda\eta'(0)}{\theta(\theta+\sigma+d)}<1,$$

*then the DFE of the Marburg disease model* (3.2)-(3.3) *always exists and is asymptotically stable.*

*Proof.* The existence result follows from the same standard theory of ODEs. With reference to [9,26], it suffices to show that all the eigenvalues, say $\lambda_i, i=1,\ldots,4$ of the Jacobian matrix $J(X_o)$ reside outside the angular sector

$$|\mathrm{Arg}\lambda_i| \leq \frac{1}{2}\gamma\pi, \quad i=1,\ldots,4,$$

which is also closed. Mathematically, it is expressed by the following constraint:

$$|\mathrm{Arg}\lambda_i| > \frac{1}{2}\gamma\pi, \quad \forall i=1,2,3,4. \tag{3.7}$$

The characteristic matrix given as

$$\Pi_J(\lambda) = \begin{pmatrix} \theta+\lambda & \beta\dfrac{\Lambda}{\theta}\eta'(0) & -(1-\nu)\zeta & 0 \\ 0 & -\beta\dfrac{\Lambda}{\theta}\eta'(0)+(\theta+\sigma+d)+\lambda & 0 & 0 \\ 0 & -\sigma & \theta+\nu+(1-\nu)\zeta+\lambda & 0 \\ 0 & d & 0 & \theta+\lambda \end{pmatrix} \tag{3.8}$$

yields the following characteristic equation:

$$(\theta+\lambda)^2\big(\theta+\nu-(1+\gamma)\zeta+\lambda\big)\left(-\beta\frac{\Lambda}{\theta}\eta'(0)+(\theta+\sigma+d)+\lambda\right)=0.$$

Hence, the eigenvalues read as

$$\lambda_{1,2}=-\theta, \quad \lambda_3=-\big(\theta+\nu+(1-\nu)\zeta\big), \quad \lambda_4=\beta\frac{\Lambda}{\theta}\eta'(0)-(\theta+\sigma+d).$$

The requested condition is met except for $\lambda_4$. Then, it becomes obvious that $\lambda_4$ verifies (3.7) if

$$\frac{\beta\Lambda\eta'(0)}{\theta} < \theta+\sigma+d,$$

which completes the proof. □

The basic reproduction number for the Marburg model (3.2)-(3.3), reads as

$$\mathcal{R}_0 = \frac{\beta\Lambda\eta'(0)}{\theta(\theta+\sigma+d)}. \tag{3.9}$$

It expresses the number of secondary Marburg infections that one infected case is going to cause in a population totally susceptible to catch MARV. Practically speaking, the Proposition 3.3 here above implies that if $\mathcal{R}_0<1$ then, the MVD will die out.

**Remark 3.1.** Note that Figs. 5 and 6 graphically show the contour plots of the basic reproduction number $\mathcal{R}_0$ seen to be varying with some sensitive parameters of the Marburg model and indicating possible dynamics of the Marburg disease. Especially, Fig. 6, from which we have the confirmation of a possibility to decrease $\mathcal{R}_0$ below the threshold of unity, with the condition of reducing the transmission rate $\beta$ while augmenting the recovery rate and improving on the case detection of symptomatic cases.

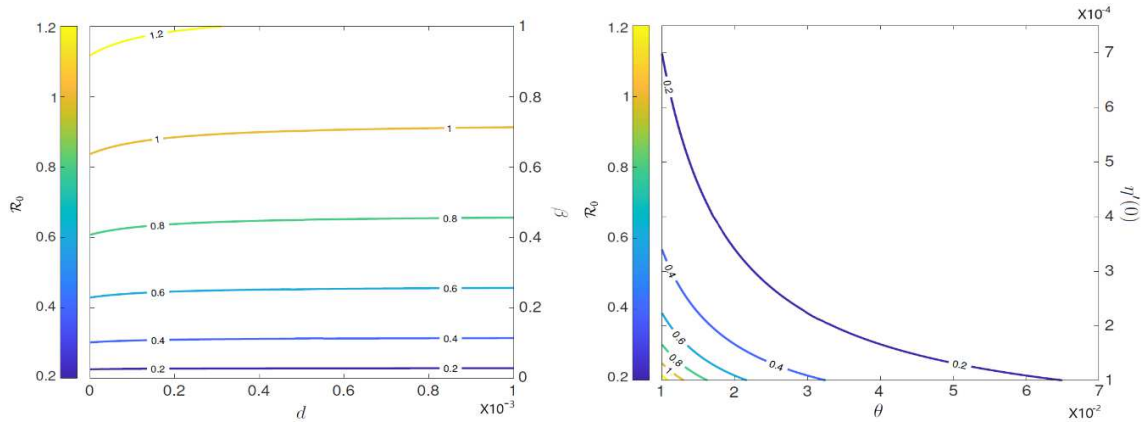


Figure 5: The two-dimensional contour plots of basic reproduction number, $\mathcal{R}_0$ as function of control parameters $d$ and $\theta$, respectively.

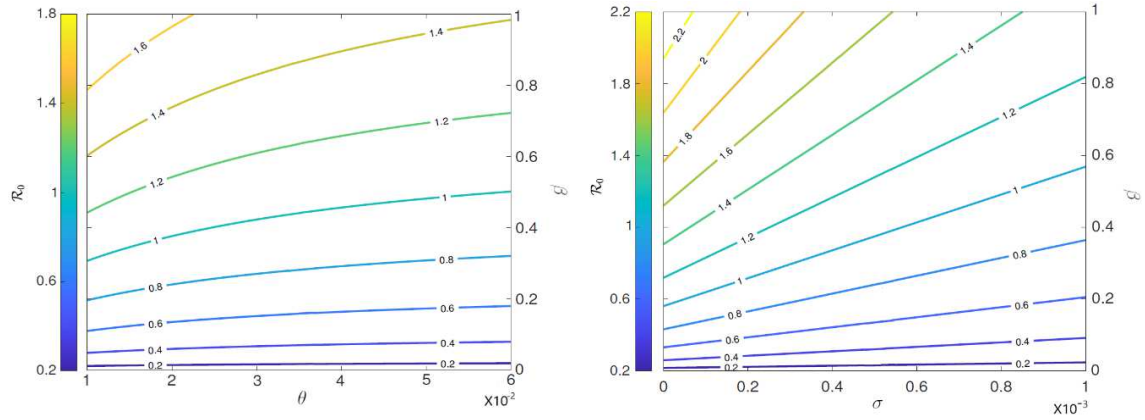


Figure 6: The two-dimensional contour plots of basic reproduction number, $\mathcal{R}_0$ as function of control parameters $\theta$ and $\sigma$, respectively.

### 3.2.2 Existence and stability results

Let us transform (3.5) into

$$\frac{1}{\varpi}=\frac{\theta(\theta+\sigma+d)}{\Lambda\beta}=\frac{\eta(I)}{I}\left(1-\frac{I}{\Xi}\right)\equiv\mathbf{m}(I), \tag{3.10}$$

where

$$\Xi=\frac{\Lambda\big(\theta+\nu+(1-\nu)\zeta\big)}{(\theta+\sigma+d)\big(\theta+\nu+(1-\nu)\zeta\big)-(1-\nu)\zeta\sigma}.$$

Then, the $I$ – solutions to (3.9) all depend on $\eta(I)$, more precisely on $\lim_{I\to 0}\eta(I)/I\equiv\mathbf{m}(0)$ and the $\mathrm{sgn}(\mathbf{m}'(I))$.

Note that $\Xi$ represents the maximum value $I_*$ can reach and $\varpi=\Lambda\beta/(\theta(\theta+\sigma+d))$ is seen as the contact reproduction number in well-known usual theory of mass action incidence in which $\eta(I)=I$. Following [9,24,26], we have the following results summarizing the conditions of existence for $X_*$.

**Proposition 3.4.** *For Marburg model* (3.2)-(3.3)*:*

1) *If $\boldsymbol{m}(0)>1/\varpi$ and $\boldsymbol{m}'(I)<0$ for all $I\in(0,\Xi)$ then, there exists one endemic equilibrium point.*
2) *If $\boldsymbol{m}(0)=0,\boldsymbol{m}''(I)<0$ on $(0,\Xi]$ and $\varpi<\varpi^*$ then, there exists no endemic equilibrium point.*
3) *If $\boldsymbol{m}(0)\leq 1/\varpi$ and $\boldsymbol{m}'(I)<0$ for all $I\in(0,\Xi)$ then, there exists no endemic equilibrium point.*
4) *If $\boldsymbol{m}(0)=0$, $\boldsymbol{m}''(I)<0$ on $(0,\Xi]$ and $\varpi=\varpi^*$ then, there exists one endemic equilibrium point.*
5) *If $\boldsymbol{m}(0)=0$, $\boldsymbol{m}''(I)<0$ on $(0,\Xi]$ and $\varpi>\varpi^*$ then, there exist two endemic equilibrium points $I_*^1$ and $I_*^2$, with $I_*^1\in(0,I_m)$ and $I_*^2\in(I_m,\Xi)$.*

In this proposition, $\varpi^*$ represents the only value of $\varpi$ satisfying the Eq. (3.10) when $I$ attains its unique maximum $I_m$ in $(0,\Xi)$.

Recalling that

$$\eta'(0)\sim\lim_{I\to 0}\frac{\eta(I)-\eta(0)}{I-0}\equiv\mathbf{m}(0),$$

and knowing that $\mathbf{m}(I)$ is positive when $I\in(0,\Xi)$, with $\mathbf{m}(\Xi)=0$, where we have taken into account the basic reproduction number $\mathcal{R}_0$ defined in (3.9). Then, from the number 1) of the Proposition 3.4 and Eq. (3.10), we can state the result.

**Corollary 3.1.** *The Marburg model* (3.2)-(3.3) *has a unique endemic equilibrium if $\mathcal{R}_0>1$, and $\boldsymbol{m}'(I)<0$ for $I\in(0,\Xi)$.*

Having provided the existence conditions for the endemic equilibrium point of the MARV model, we can now investigate the stability.

In the following lines, we analyze the conditions of stability for the endemic equilibrium $X_*=(S_*,I_*,R_*,N_*)$ using the linearized system of (3.2)-(3.3) around $X_*$. This development leads to the Jacobian matrix

$$J(X_*)=\begin{pmatrix}-\beta\eta(I_*)-\theta & -\beta S_*\eta'(I_*) & (1-\nu)\zeta & 0\\ \beta\eta(I_*) & \beta S_*\eta'(I_*)-(\theta+\sigma+d) & 0 & 0\\ 0 & \sigma & -(\theta+\nu)-(1-\nu)\zeta & 0\\ 0 & -d & 0 & -\theta\end{pmatrix}. \tag{3.11}$$

We can look at the eigenvalues $\lambda_r, r=1,2,3,4$, using characteristic equation

$$\begin{vmatrix} \beta\eta(I_*)+\theta+\lambda & \beta S_*\eta'(I_*) & -(1-\nu)\zeta & 0 \\ -\beta\eta(I_*) & -\beta S_*\eta'(I_*)+(\theta+\sigma+d)+\lambda & 0 & 0 \\ 0 & -\sigma & (\theta+\nu)+(1-\nu)\zeta+\lambda & 0 \\ 0 & d & 0 & \theta+\lambda \end{vmatrix}=0, \quad (3.12)$$

which gives

$$C(\theta+\lambda)\left(\lambda^3+C_1\lambda^2+C_2\lambda+C_3\right)=0 \quad (3.13)$$

with

$$\begin{aligned} C_1 &= \beta\eta(I_*)+2\theta+(1-\nu)\zeta+(\theta+\sigma+d)\left(1-I_*\frac{\eta'(I_*)}{\eta(I_*)}\right), \\ C_2 &= \beta(\theta+\sigma+d)\eta'(I_*)I_*+\left(\theta+\nu+(1-\nu)\zeta\right)\left(\beta\eta(I_*)+2\theta\right) \\ &\quad +\left(\beta\eta(I_*)+2\theta+\nu+(1-\nu)\zeta\right)(\theta+\sigma+d)\left(1-I_*\frac{\eta'(I_*)}{\eta(I_*)}\right), \\ C_3 &= \beta(\theta+\sigma+d)\left(\theta+\nu+(1-\nu)\zeta\right)\eta'(I_*)I_*-\beta\eta(I_*)\sigma(1-\nu)\zeta \\ &\quad +\left(\beta\eta(I_*)+\theta\right)\left(\theta+\nu+(1-\nu)\zeta\right)(\theta+\sigma+d)\left(1-I_*\frac{\eta'(I_*)}{\eta(I_*)}\right). \end{aligned} \quad (3.14)$$

It appears clearly that $C_1, C_2$, and $C_3$ depend on the function $\eta(I)$. Because the eigenvalue $\lambda=-\theta$ is not positive, we can only rely on the roots of

$$P(\lambda)=\lambda^3+C_1\lambda^2+C_2\lambda+C_3=0$$

defined in (3.13) to establish the stability results using the extended Routh-Hurwitz criteria as proposed in [2]. Hence, we have proved the following results.

**Corollary 3.2.** *The endemic equilibrium $X_*$ of the MARV model* (3.2)-(3.3) *is asymptotically stable if one of the following conditions hold:*

1) $C_1\geq 0, C_2\geq 0, C_3>0, \Pi_P<0$, *and* $0<\gamma\leq 2/3$,
2) $C_1<0, C_2<0, \Pi_P<0$, *and* $2/3<\gamma\leq 1$,
3) $C_1>0, C_3>0, C_1C_2>C_3$, *and* $\Pi_P>0$,

*where $\Pi_P$ is the polynomial $P(\lambda)$'s discriminant.*

The bifurcation analysis are depicted in Figs. 13 and 14 showing condition for the model to have forward and backward bifurcations respectively and show that the model contains a backward bifurcation under certain conditions.

# 4 Impact of Mittag-Leffler kernel

The Mittag-Leffler function, a function arising naturally in the expression of solutions to differential and integral equations of fractional order, is also highly important in relaxation processes. Other works have shown its importance in applied sciences [13,14,18,19]. The function has attracted a growing attention of scientists in the past decades thanks to its capability of describing conventional and non conventional real life phenomena, in an accurate manner.

In this section, we generalize the Marburg model by including the Mittag-Leffler kernel to get

$$\begin{cases} {}^{abc}D_t^{\gamma} S = \Lambda - \beta S\eta(I) + (1-\nu)\zeta R - \theta S, \\ {}^{abc}D_t^{\gamma} I = \beta S\eta(I) - (\theta+\sigma+d)I, \\ {}^{abc}D_t^{\gamma} R = \sigma I - (\theta+\nu)R - (1-\nu)\zeta R, \\ {}^{abc}D_t^{\gamma} U = \nu R - \theta U \end{cases} \tag{4.1}$$

with initial conditions

$$S(0)=S_0, \quad I(0)=I_0, \quad R(0)=R_0, \quad U(0)=U_0, \tag{4.2}$$

where ${}^{abc}D_t^{\gamma}$ is the Atangana-Baleanu derivative known to incorporate the Mittag-Leffler kernel and mathematically defined as

$${}^{abc}D_t^{\gamma} u(t) = \frac{\mathbf{B}(\gamma)}{(1-\gamma)} \int_0^t \frac{du}{d\xi}(\xi) E_{\gamma}\left[-\frac{\gamma(t-\xi)^{\gamma}}{1-\gamma}\right] d\xi, \quad 0<\gamma\leq 1. \tag{4.3}$$

We associate the ${}^{abc}D_t^{\gamma}$-operator with its anti-derivative given by

$${}^{ab}I^{\gamma} u(t) = \frac{1-\gamma}{\mathbf{B}(\gamma)} u(t) + \frac{\gamma}{\mathbf{B}(\gamma)} \frac{1}{\Gamma(\gamma)} \int_0^t (t-\xi)^{\gamma-1} u(\xi) d\xi, \quad t>0. \tag{4.4}$$

Before going further, we state the following results.

**Lemma 4.1** ([7]). *If $\gamma \in (0,1]$ then,*

$${}^{ab}I^{\gamma}\,{}^{abc}D_t^{\gamma} u(t) = u(t) - b_0. \tag{4.5}$$

*Hence, the following problem:*

$$\begin{cases} {}^{abc}D_t^{\gamma} u(t) = G(t), \\ u(0) = u_0 \end{cases} \tag{4.6}$$

*has the solution expressed as*

$$u(t) = u_0 + \frac{1-\gamma}{\mathbf{B}(\gamma)} G(t) + \frac{\gamma}{\mathbf{B}(\gamma)} \frac{1}{\Gamma(\gamma)} \int_0^t (t-\xi)^{\gamma-1} G(\xi) d\xi. \tag{4.7}$$

**Theorem 4.1** ([28]). *Let us consider the following system with derivative of fractional-order:*

$$\begin{cases} {}^{abc}D_t^{\gamma}u(t) = G\big(u(t)\big), \quad 0<\gamma\leq 1, \\ u(t_0) = u_0 \in \mathbb{R}^m \end{cases} \tag{4.8}$$

*with* $u(t) = (u_1, u_2, \cdots, u_m(t)) \in \mathbb{R}^m$ *and* $z : [G_1, G_2, \cdots, G_m]^{\top} : \mathbb{R}^m \to \mathbb{R}^m$. *Hence, solutions to* $G(z(t)) = 0$ *are defined to be the equilibria for the model. An equilibrium point* $\boldsymbol{q}$ *is said to be locally asymptotically stable if and only if all eigenvalues* $z_i$ *of the Jacobian* $J = \partial G/\partial u$, *evaluated at* $\boldsymbol{q}$ *verify the inequality* $|\mathrm{Arg}(z_i)| > \gamma\pi/2$.

With these two results in mind, the Marburg model (4.1) can be transformed into

$$\begin{aligned} {}^{abc}D_t^{\gamma}S &= G_1(t,S,I,R,U), \\ {}^{abc}D_t^{\gamma}I &= G_2(t,S,I,R,U), \\ {}^{abc}D_t^{\gamma}R &= G_3(t,S,I,R,U), \\ {}^{abc}D_t^{\gamma}U &= G_4(t,S,I,R,U) \end{aligned} \tag{4.9}$$

with

$$\begin{aligned} G_1(t,S,I,R,U) &= \Lambda - \beta S\eta(I) + (1-\nu)\zeta R - \theta S, \\ G_2(t,S,I,R,U) &= \beta S\eta(I) - (\theta+\sigma+d)I, \\ G_3(t,S,I,R,U) &= \sigma I - (\theta+\nu)R - (1-\nu)\zeta R, \\ G_4(t,S,I,R,U) &= \nu R - \theta U. \end{aligned} \tag{4.10}$$

Whence, with reference to the fractional system (4.1), we consider the nonlinear system given by

$$\begin{cases} {}^{abc}D_t^{\gamma}u(t) = \mathcal{Y}\big(t,u(t)\big), \quad 0\leq t\leq b, \quad 0<\gamma\leq 1, \\ u(0) = u_0 \geq 0 \end{cases} \tag{4.11}$$

with

$$\begin{cases} u(t) = (S,I,R,U)^{\top}, \\ u_0 = (S_0,I_0,R_0,U_0)^{\top}, \\ \mathcal{Y}\big(t,u(t)\big) = \big(G_j(t,S,I,R,U)\big)^{\top}, \quad j=1,\ldots,4. \end{cases} \tag{4.12}$$

In the following lines,

$$\|u\| = \sup_{t\in[0,e]} |u(t)|$$

defines a norm in the Banach space denoted by $\mathbf{A} = \mathcal{C}([0,e],\mathbb{R}^4)$ with $|u(t)| = |S| + |I| + |R| + |U|$, $S, I, R, U \in \mathcal{C}[0,e]$ and $\mathcal{Y} : [0,e]\times\mathbb{R}^4 \to \mathbb{R}$ a continuous function.

With reference to Lemma 4.1 and Theorem 4.1, the problem (4.11) takes the form of an integral equation that reads as

$$u(t) = u_0 + \frac{1-\gamma}{\mathbf{B}(\gamma)}\mathcal{Y}\big(t,u(t)\big) + \frac{\gamma}{\mathbf{B}(\gamma)}\frac{1}{\Gamma(\gamma)}\int_0^t (t-\xi)^{\gamma-1}\mathcal{Y}\big(\xi,u(\xi)\big)d\xi. \tag{4.13}$$

At this stage, using Eq. (4.13), the operator $\mathbf{O}:\mathbf{A}\to\mathbf{A}$ can be defined as

$$(\mathbf{O}u)(t)=u_0+\frac{1-\gamma}{\mathbf{B}(\gamma)}\mathcal{Y}\big(t,u(t)\big)+\frac{\gamma}{\mathbf{B}(\gamma)}\frac{1}{\Gamma(\gamma)}\int_0^t(t-\xi)^{\gamma-1}\mathcal{Y}\big(\xi,u(\xi)\big)d\xi. \tag{4.14}$$

**Remark 4.1.** Recall that, a solution to the model (4.11) exist if and only if the operator **O** has a fixed point.

The existence of a solution is a direct consequence of the notion of Schauder fixed point theorem [31].

**Proposition 4.1.** *Let us consider:*

*($\mathcal{H}_1$) There is $\alpha_1,\alpha_2\in\boldsymbol{A}$ so that*

$$\alpha_1^*=\sup_{t\in[0,e]}|\alpha_1(t)|,\quad \alpha_2^*=\sup_{t\in[0,e]}|\alpha_2(t)|<1,$$

*and for every $t\in[0,e],u\in\boldsymbol{A}$,*

$$\big|\mathcal{Y}\big(t,u(t)\big)\big|\leq\alpha_1(t)+\alpha_2(t)|u(t)|.$$

*Hence, there exists at least one solution to the problem* (4.11) (*and therefore the system* (4.1))

*Proof.* To prove of the proposition, we proceed as follows.

1. We start by proving that the operator **O** continuous. In fact, let a sequence $u_n\in\mathbf{A}$ defined as $u_n\to u$ and take $t\in[0,e]$. Hence, we get

$$\begin{aligned}&|(\mathbf{O}u_n)(t)-(\mathbf{O}u)(t)|\\ &\leq\frac{1-\gamma}{\mathbf{B}(\gamma)}\big|\mathcal{Y}\big(t,u_n(t)\big)-\mathcal{Y}\big(t,u(t)\big)\big|\\ &\quad+\frac{\gamma}{\mathbf{B}(\gamma)}\frac{1}{\Gamma(\gamma)}\int_0^t(t-\xi)^{\gamma-1}\big|\mathcal{Y}\big(\xi,u_n(\xi)\big)-\mathcal{Y}\big(\xi,u(\xi)\big)\big|d\xi\\ &\leq\left(\frac{1-\gamma}{\mathbf{B}(\gamma)}+\frac{e^\gamma}{\mathbf{B}(\gamma)\Gamma(\gamma)}\right)\big\|\mathcal{Y}\big(\cdot,u_n(\cdot)\big)-\mathcal{Y}\big(\cdot,u(\cdot)\big)\big\|.\end{aligned} \tag{4.15}$$

   Using the continuity property of $\mathcal{Y}$, we have $\|\mathbf{O}u_n-\mathbf{O}u\|\longrightarrow 0$ as $n\to+\infty$.

2. Secondly, we prove that operator **O** maps bounded sets into bounded sets. Let $\mathbf{E}_r$ be the set given as $\mathbf{E}_r=\{u\in\mathbf{A}:\|u\|\leq r\}$, then, we just need to prove existence of a coefficient $\mathcal{M}>0$ so that $\|\mathbf{O}u\|\leq\mathcal{M}$. Then,

$$|(\mathbf{O}u)(t)|\leq\|u_0\|+\frac{1-\gamma}{\mathbf{B}(\gamma)}\big|\mathcal{Y}\big(t,u(t)\big)\big|+\frac{\gamma}{\mathbf{B}(\gamma)}\frac{1}{\Gamma(\gamma)}\int_0^t(t-\xi)^{\gamma-1}\big|\mathcal{Y}\big(\xi,u(\xi)\big)\big|d\xi, \tag{4.16}$$

   now referring to the condition $(\mathcal{H}_1)$, leads to

$$\big|\mathcal{Y}\big(t,u(t)\big)\big|\leq\alpha_1(t)+\alpha_2(t)|u(t)|.$$

Thus,

$$\begin{aligned}|(\mathbf{O}u)(t)| &\leq \|u_0\| + \frac{1-\gamma}{\mathbf{B}(\gamma)}(\alpha_1^* + \alpha_2^*\|u\|) + \frac{e^\gamma}{\mathbf{B}(\gamma)}\frac{1}{\Gamma(\gamma)}(\alpha_1^* + \alpha_2^*\|u\|)\\ &\leq \|u_0\| + \frac{\alpha_1^*}{\mathbf{B}(\gamma)}\left((1-\gamma) + \frac{e^\gamma}{\Gamma(\gamma)}\right) + \frac{\alpha_2^*}{\mathbf{B}(\gamma)}\left((1-\gamma) + \frac{e^\gamma}{\Gamma(\gamma)}\right)\|u\|\\ &\leq \|u_0\| + \frac{\alpha_1^*}{\mathbf{B}(\gamma)}\left((1-\gamma) + \frac{e^\gamma}{\Gamma(\gamma)}\right) + \frac{\alpha_2^* r}{\mathbf{B}(\gamma)}\left((1-\gamma) + \frac{e^\gamma}{\Gamma(\gamma)}\right)\\ &\leq \mathcal{M} < +\infty. \end{aligned} \tag{4.17}$$

3. Thirdly, we prove that operator **O** maps bounded sets to equicontinuous sets. For $t_1, t_2 \in [0,e]$ with $t_1 \geq t_2$ and $u \in \mathbf{E}_r$, we get

$$\begin{aligned}&|(\mathbf{O}u)(t_1) - (\mathbf{O}u)(t_2)|\\ &\leq \left| \frac{\gamma}{\mathbf{B}(\gamma)}\frac{1}{\Gamma(\gamma)}\int_0^{t_1}(t_1-\xi)^{\gamma-1}\mathcal{Y}\big(\xi,u(\xi)\big)d\xi \right.\\ &\quad \left. - \frac{\gamma}{\mathbf{B}(\gamma)}\frac{1}{\Gamma(\gamma)}\int_0^{t_2}(t_2-\xi)^{\gamma-1}\mathcal{Y}\big(\xi,u(\xi)\big)d\xi \right|\\ &\leq \frac{\gamma}{\mathbf{B}(\gamma)}\frac{1}{\Gamma(\gamma)}\int_0^{t_1}\left[(t_1-\xi)^{\gamma-1} - (t_2-\xi)^{\gamma-1}\right]\left|\mathcal{Y}\big(\xi,u(\xi)\big)\right|d\xi\\ &\quad + \frac{\gamma}{\mathbf{B}(\gamma)}\frac{1}{\Gamma(\gamma)}\int_{t_1}^{t_2}(t_2-\xi)^{\gamma-1}\left|\mathcal{Y}\big(\xi,u(\xi)\big)\right|d\xi\\ &\leq \frac{(\alpha_1^* + \alpha_2^* r)}{\mathbf{B}(\gamma)\Gamma(\gamma)}\left[2(t_1-t_2)^\gamma + \left(t_2^\gamma - t_2^\gamma\right)\right] \longrightarrow 0 \quad \text{as} \quad t_1 \to t_2. \end{aligned} \tag{4.18}$$

Whence, the full continuity property of **O** follows from the three steps above and the Arzelá-Ascoli theorem.

4. Lastly, we prove that operator **O** represents a priori bound. To achieve it, we let

$$\mathbf{A}_1 = \{u \in \mathbf{A} : u = \pi(\mathbf{O}u), 0 < \pi < 1\}.$$

So, we just need to prove that $\mathbf{A}_1$ is a bounded set. Indeed, considering any $t \in [0,e]$ and $u \in \mathbf{A}_1$ yields

$$\begin{aligned}u(t) = \pi\Bigg[&u_0 + \frac{1-\gamma}{\mathbf{B}(\gamma)}\mathcal{Y}\big(t,u(t)\big)\\ &+ \frac{\gamma}{\mathbf{B}(\gamma)}\frac{1}{\Gamma(\gamma)}\int_0^t(t-\xi)^{\gamma-1}\mathcal{Y}\big(\xi,u(\xi)\big)d\xi\Bigg], \quad 0 < \pi < 1. \end{aligned} \tag{4.19}$$

Referring to $(\mathcal{H}_1)$, leads to

$$\begin{aligned}|u(t)| &\leq |(\mathbf{O}u)(t)|\\ &\leq \|u_0\| + \frac{\alpha_1^*}{\mathbf{B}(\gamma)}\left((1-\gamma) + \frac{e^\gamma}{\Gamma(\gamma)}\right) + \frac{\alpha_2^* r}{\mathbf{B}(\gamma)}\left((1-\gamma) + \frac{e^\gamma}{\Gamma(\gamma)}\right) < +\infty. \end{aligned} \tag{4.20}$$

Hence, we obtain the expected result as a consequence of Schauder fixed point theorem [31] via it particular version, the Schaefer's fixed point theorem. Which completes the proof. □

The proof of uniqueness results for the solution can be achieved using the Banach contraction principle as shown in the following lines.

**Proposition 4.2.** *Let us consider*

*($\mathcal{H}_2$) There is $\delta>0$ (constant) so that*

$$\mathcal{Y}\big(t,u_1(t)\big)-\mathcal{Y}\big(t,u_2(t)\big)\leq\delta|u_1(t)-u_2(t)|$$

*for every $t\in[0,e]$ and $u_1,u_2\in\boldsymbol{A}$.*

*Hence, if the inequality*

$$\left(\frac{1-\gamma}{\mathbf{B}(\gamma)}+\frac{e^{\gamma}}{\mathbf{B}(\gamma)\Gamma(\gamma)}\right)\delta<1$$

*holds, then the solution to the problem* (4.11) *(and therefore the system* (4.1)*) is unique.*

*Proof.* Making use of

$$\sup_{t\in[0,e]}|\mathcal{Y}(t,0)|=\rho<+\infty,\quad r\geq\frac{\rho\Theta+\|u_0\|}{1-\delta\Theta},$$

we can define a neighborhood with radius denoted by $r$. Then, we prove that $\mathbf{O}\mathbf{E}_r\subset\mathbf{E}_r$, where $\mathbf{E}_r=\{u\in\mathbf{A}:\|u\|\leq r\}$. So, for a $u\in\mathbf{E}_r$ and $t\in[0,e]$, we have

$$\begin{aligned}
|(\mathbf{O}u)(t)|&\leq\sup_{t\in[0,e]}\left(|u_0|+\frac{1-\gamma}{\mathbf{B}(\gamma)}|\mathcal{Y}\big(t,u(t)\big)|+\frac{\gamma}{\mathbf{B}(\gamma)}\frac{1}{\Gamma(\gamma)}\int_0^t(t-\xi)^{\gamma-1}|\mathcal{Y}\big(\xi,u(\xi)\big)|d\xi\right)\\
&\leq\|u_0\|+\frac{1-\gamma}{\mathbf{B}(\gamma)}|\mathcal{Y}\big(t,u(t)\big)|(e)+\frac{\gamma}{\mathbf{B}(\gamma)}\frac{1}{\Gamma(\gamma)}\int_0^e(e-\xi)^{\gamma-1}|\mathcal{Y}\big(\xi,u(\xi)\big)|d\xi\\
&\leq\|u_0\|+\frac{1-\gamma}{\mathbf{B}(\gamma)}\big(|\mathcal{Y}\big(t,u(t)\big)-\mathcal{Y}(t,0)|+|\mathcal{Y}(t,0)|\big)\\
&\quad+\frac{\gamma}{\mathbf{B}(\gamma)}\frac{1}{\Gamma(\gamma)}\int_0^e(e-\xi)^{\gamma-1}\big[|\mathcal{Y}\big(\xi,u(\xi)\big)-\mathcal{Y}(t,0)|+\mathcal{Y}(t,0)|\big]d\xi\\
&\leq\|u_0\|+(\delta\|u\|+\rho)\left\{\frac{1-\gamma}{\mathbf{B}(\gamma)}+\frac{e^{\gamma}}{\mathbf{B}(\gamma)\Gamma(\gamma)}\right\}\\
&\leq\|u_0\|+(\delta\|u\|+\rho)\Theta\leq r.
\end{aligned}\tag{4.21}$$

Thus, $\mathbf{O}\mathbf{E}_r\subset\mathbf{E}_r$. Moreover, let $u_1,u_2\in\mathbf{A}$, then for each $t\in[0,e]$, we have

$$\begin{aligned}
&|(\mathbf{O}u_1)(t)-(\mathbf{O}u_2)(t)|\\
&\leq\frac{1-\gamma}{\mathbf{B}(\gamma)}|\mathcal{Y}\big(t,u_1(t)\big)-\mathcal{Y}(t,u_2)|
\end{aligned}$$

$$+\frac{\gamma}{\mathbf{B}(\gamma)}\frac{1}{\Gamma(\gamma)}\int_0^t (t-\xi)^{\gamma-1}\left|\mathcal{Y}\left(\xi,u_1(\xi)\right)-\mathcal{Y}\left(\xi,u_2(\xi)\right)\right|d\xi$$
$$\leq \delta\left(\frac{1-\gamma}{\mathbf{B}(\gamma)}+\frac{e^{\gamma}}{\mathbf{B}(\gamma)\Gamma(\gamma)}\right)\|u_1-u_2\|. \tag{4.22}$$

It follows, the hypothesis of the proposition above, that the operator **O** is contractive. Thus, the Banach contraction principle yields the desired uniqueness result, which completes the proof. □

## 5 Numerical approximation scheme

We provide in this section a numerical technique to address the solvability of fractional system (4.1) similar to the one proposed in [34]. Recall that a huge number of other real world problems have successfully been described by many authors using numerical schemes based on the same numerical iterative principle [1, 3, 5, 7, 8, 11, 20, 21] and references therein.

Applying the Atangana-Baleanu antiderivative given in (4.4) on both sides of the MARV fractional system (4.1), using the initial conditions and Lemma 4.1 lead to the system

$$\begin{aligned}
S(t)&=S_0+\frac{1-\gamma}{\mathbf{B}(\gamma)}\mathcal{Z}_1\left(t,S(t)\right)+\frac{\gamma}{\mathbf{B}(\gamma)}\frac{1}{\Gamma(\gamma)}\int_0^t (t-\xi)^{\gamma-1}\mathcal{Z}_1\left(\xi,S(\xi)\right)d\xi,\\
I(t)&=I_0+\frac{1-\gamma}{\mathbf{B}(\gamma)}\mathcal{Z}_2\left(t,I(t)\right)+\frac{\gamma}{\mathbf{B}(\gamma)}\frac{1}{\Gamma(\gamma)}\int_0^t (t-\xi)^{\gamma-1}\mathcal{Z}_2\left(\xi,I(\xi)\right)d\xi,\\
R(t)&=R_0+\frac{1-\gamma}{\mathbf{B}(\gamma)}\mathcal{Z}_3\left(t,R(t)\right)+\frac{\gamma}{\mathbf{B}(\gamma)}\frac{1}{\Gamma(\gamma)}\int_0^t (t-\xi)^{\gamma-1}\mathcal{Z}_3\left(\xi,R(\xi)\right)d\xi,\\
U(t)&=U_0+\frac{1-\gamma}{\mathbf{B}(\gamma)}\mathcal{Z}_4\left(t,U(t)\right)+\frac{\gamma}{\mathbf{B}(\gamma)}\frac{1}{\Gamma(\gamma)}\int_0^t (t-\xi)^{\gamma-1}\mathcal{Z}_4\left(\xi,U(\xi)\right)d\xi
\end{aligned} \tag{5.1}$$

with $\mathcal{Z}_i, i=1,2,3,4$ referring to $G_i, i=1,2,3,4$ defined in (4.10). The recursive scheme for the $S(t)$-equation of the system (5.1) is given by the formula

$$S(t)=S_0+\frac{1-\gamma}{\mathbf{B}(\gamma)}\mathcal{Z}_1\left(t,S(t)\right)+\frac{\gamma}{\mathbf{B}(\gamma)}\frac{1}{\Gamma(\gamma)}\int_0^t (t-\xi)^{\gamma-1}\mathcal{Z}_1\left(\xi,S(\xi)\right)d\xi, \tag{5.2}$$

and substitution of $t=t_{n+1}, n=0,1,\ldots$ into Eq. (5.2), leads to

$$\begin{aligned}
S(t_{n+1})&=S(t_0)+\frac{1-\gamma}{\mathbf{B}(\gamma)}\mathcal{Z}_1\left(t_n,S(t_n)\right)+\frac{\gamma}{\mathbf{B}(\gamma)}\frac{1}{\Gamma(\gamma)}\int_0^{t_{n+1}} (t_{n+1}-\xi)^{\gamma-1}\mathcal{Z}_1\left(\xi,S(\xi)\right)d\xi \qquad (5.3)\\
&=S(t_0)+\frac{1-\gamma}{\mathbf{B}(\gamma)}\mathcal{Z}_1\left(t_n,S(t_n)\right)+\frac{\gamma}{\mathbf{B}(\gamma)}\frac{1}{\Gamma(\gamma)}\sum_{r=0}^{n}\int_{t_r}^{t_{r+1}} (t_{n+1}-\xi)^{\gamma-1}\mathcal{Z}_1\left(\xi,S(\xi)\right)d\xi.
\end{aligned}$$

We can approximate $\mathcal{Z}_1(\xi,S(\xi))$ in the $[t_r,t_{r+1}]$ interval with $t_r=rh$ to get

$$\mathcal{Z}_1(\xi,S(\xi))\cong\frac{\mathcal{Z}_1\big(t_r,S(t_r)\big)}{h}(t-t_{r-1})-\frac{\mathcal{Z}_1\big(t_{r-1},S(t_{r-1})\big)}{h}(t-t_r),$$

equivalently

$$\begin{aligned}S(t_{n+1})=S(t_0)+\frac{1-\gamma}{\mathbf{B}(\gamma)}\mathcal{Z}_1\big(t_n,S(t_n)\big)\\+\frac{\gamma}{\mathbf{B}(\gamma)}\frac{1}{\Gamma(\gamma)}\sum_{r=0}^{n}\Bigg(\frac{\mathcal{Z}_1\big(t_r,S(t_r)\big)}{h}\int_{t_r}^{t_{r+1}}(t-t_{r-1})(t_{n+1}-\xi)^{\gamma-1}d\xi\\-\frac{\mathcal{Z}_1\big(t_{r-1},S(t_{r-1})\big)}{h}\int_{t_r}^{t_{r+1}}(t-t_r)(t_{n+1}-\xi)^{\gamma-1}d\xi\Bigg),\end{aligned}\tag{5.4}$$

where we have used the Lagrange interpolation polynomial method. Now, integrating by parts and the substituting $t_r=rh$ into (5.4) give

$$\begin{aligned}S(t_{n+1})=S(t_0)+\frac{1-\gamma}{\mathbf{B}(\gamma)}\mathcal{Z}_1\big(t_n,S(t_n)\big)\\+\frac{\gamma}{\mathbf{B}(\gamma)}\sum_{r=0}^{n}\Bigg[\frac{h^\gamma\mathcal{Z}_1\big(t_r,S(t_r)\big)}{\Gamma(\gamma+2)}\big[(n+1-r)^\gamma(n-r+2+\gamma)-(n-r)^\gamma(n-r+2+2\gamma)\big]\\-\frac{h^\gamma\mathcal{Z}_1\big(t_{r-1},S(t_{r-1})\big)}{\Gamma(\gamma+2)}\big[(n+1-r)^{\gamma+1}-(n-r)^\gamma(n-r+1+\gamma)\big]\Bigg],\end{aligned}\tag{5.5}$$

which is the desired iteration form. We can proceed in a similar way to obtain the same iteration scheme for the $I(t),R(t)$ and $U(t)$-equation of the system (5.1) respectively given by

$$\begin{aligned}I(t_{n+1})=I(t_0)+\frac{1-\gamma}{\mathbf{B}(\gamma)}\mathcal{Z}_2\big(t_n,I(t_n)\big)\\+\frac{\gamma}{\mathbf{B}(\gamma)}\sum_{r=0}^{n}\Bigg[\frac{h^\gamma\mathcal{Z}_2\big(t_r,I(t_r)\big)}{\Gamma(\gamma+2)}\big[(n+1-r)^\gamma(n-r+2+\gamma)-(n-r)^\gamma(n-r+2+2\gamma)\big]\\-\frac{h^\gamma\mathcal{Z}_2\big(t_{r-1},I(t_{r-1})\big)}{\Gamma(\gamma+2)}\big[(n+1-r)^{\gamma+1}-(n-r)^\gamma(n-r+1+\gamma)\big]\Bigg],\end{aligned}\tag{5.6}$$

$$\begin{aligned}R(t_{n+1})=R(t_0)+\frac{1-\gamma}{\mathbf{B}(\gamma)}\mathcal{Z}_3\big(t_n,R(t_n)\big)\\+\frac{\gamma}{\mathbf{B}(\gamma)}\sum_{r=0}^{n}\Bigg[\frac{h^\gamma\mathcal{Z}_3\big(t_r,R(t_r)\big)}{\Gamma(\gamma+2)}\big[(n+1-r)^\gamma(n-r+2+\gamma)-(n-r)^\gamma(n-r+2+2\gamma)\big]\\-\frac{h^\gamma\mathcal{Z}_3\big(t_{r-1},R(t_{r-1})\big)}{\Gamma(\gamma+2)}\big[(n+1-r)^{\gamma+1}-(n-r)^\gamma(n-r+1+\gamma)\big]\Bigg],\end{aligned}\tag{5.7}$$

$$U(t_{n+1}) = U(t_0) + \frac{1-\gamma}{\mathbf{B}(\gamma)}\mathcal{Z}_4\big(t_n, U(t_n)\big) \tag{5.8}$$
$$+ \frac{\gamma}{\mathbf{B}(\gamma)}\sum_{r=0}^{n}\left[\frac{h^\gamma \mathcal{Z}_4\big(t_r, U(t_r)\big)}{\Gamma(\gamma+2)}\big[(n+1-r)^\gamma(n-r+2+\gamma)-(n-r)^\gamma(n-r+2+2\gamma)\big]\right.$$
$$\left. - \frac{h^\gamma \mathcal{Z}_4(t_{r-1}, U(t_{r-1}))}{\Gamma(\gamma+2)}\big[(n+1-r)^{\gamma+1}-(n-r)^\gamma(n-r+1+\gamma)\big]\right].$$

In order to perform some numerical simulations of the MARV model (4.1), we consider the parameters presented in the Table 1. Recall the nonlinear incidence $\eta(I) = I^k/(1+k_1 I^{\tilde{k}})$, $k, \tilde{k} > 0, k_1 \geq 0$, and we limit our analysis to the case $k_1 = 0$. The nonlinear incidence reduces to $\eta(I) = I^k$. Implementing the scheme described here above, we can perform some numerical representations as depicted in Figs. 12 and 13 where we can see three scenarios related to different values of the parameter $\gamma$.

Each case show the dynamic for three values of the parameter $\gamma$, which are $\gamma = 0.8, 0.9$ and 1. We observe similar trajectories reflecting the usual threshold behavior. In Figs. 15-16, for the nonlinear incidence's coefficient $k = 2$ and the transmission parameter $\beta = 0.01$, the dynamic of Marburg system (4.1) converges to the DFE point situated at $X_o = (6000, 0, 0, 6000)$. The same scenario is shown in Figs. 17-18 for the nonlinear incidence's coefficient $k = 2$ and the transmission parameter $\beta = 0.01$, where the dynamic of Marburg system (4.1) converges to the endemic equilibrium situated at $X_* = (9.9, 7.2, 5.3, 5748)$ and verifies the condition of Proposition 3.4.

Table 1: Descriptions with values for the parameters of the MARV system (4.1).

| Parameters' symbols | Description | Estimation and range[1)] |
|---|---|---|
| $\Lambda$ | Recruitment rate by susceptible people in the region | 60 (day)$^{-1}$ |
| $\beta$ | Transmission coefficient | Not constant |
| $\nu$ | Proportion of recovered individuals that become immunized | 0.05 |
| $\zeta$ | Rate at which recovered people go back to susceptible class | 0.08 |
| $\theta$ | Non-Marburg-disease related death rate | 0.01 |
| $d$ | Marburg related death rate | 0.6 |
| $\sigma$ | Recovery rate from Marburg | 0.1 |
| $k$ | Symbolizing the non-linear incidence | 2 |

[1)]Sources: [36], https://www.who.int/emergencies/disease-outbreak-news/item/2021-DON331.

## 6 Discussion and concluding remarks

The main focus in this paper have been about analyzing a Marburg epidemic model in which the transmission is nonlinear and represented by the non-linear function $\eta$. The

well-posedness of the model has been established before studying conditions for the boundedness and dissipativity results. Then, we have intensively studied the stability of equilibria of the generalized MARV models (2.1) and (4.1) and it appears that these models show some reliable stability under suitable conditions. The bifurcation dynamics depicted in Figs. 7 and 8 show the type of stability applicable to the models. For instance, the type transcritical shown in Fig. 7 indicates how an exchange of stability can happen between the endemic equilibrium point and the DFE, while in Fig. 8, it is rather a backward bifurcation indicating that the well known classical epidemiological condition for the MVD to die out ($\mathcal{R}_0 < 1$) is not sufficient anymore, but remains necessary. Other stability scenarios are shown in Fig. 9-11 for the MARV model (2.1) and Fig. 12-14 for the MARV model (4.1). In Fig. 9, we have the possible existence of globally stability for the DFE $X_o$ of the model (2.1), when $\mathcal{R}_0 < 1$, $(0.3813)$ and $\beta = 0.01$. In Fig. 10, we have the possible existence of stability for two equilibria: The DFE $X_o$ and the endemic equilibrium $X_1 = (8.2,15.9,6.0,5801)$, and existence of instability for the endemic equilibrium $X_2 = (281,1,9.1,7.1,5777)$ of the model (2.1), when $\mathcal{R}_0 < 1$, $(0.7433)$ and $\beta = 0.3$ and $k = 0.4$. In Fig. 11, we have the possible existence of globally stability for the endemic equilibrium $X_* = (711.1,12.2,5.8,5871)$ and instability for the DFE $X_o$ of the model (2.1), with $\mathcal{R}_0 > 1$, $(1.0074)$ and $\beta = 1.3$ and $k = 5 \times 10^{-2}$.

The stability scenarios for the model (4.1) with Mittag-Leffler kernel is depicted in Figs. 12-14 and we observe similar stability dynamics as those shown in Figs. 9-11 re-

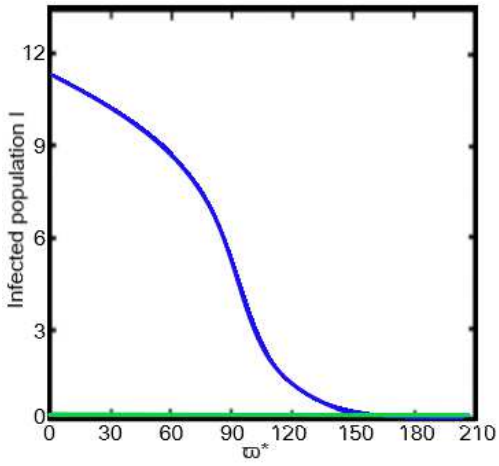


Figure 7: Bifurcation diagram for Marburg disease (2.1). The values of the parameter used here are taken from the Table 1 below. The bifurcation depicted here is of type transcritical and it indicates an exchange of stability between the endemic equilibrium point (blue line) and the disease free equilibrium (green line).

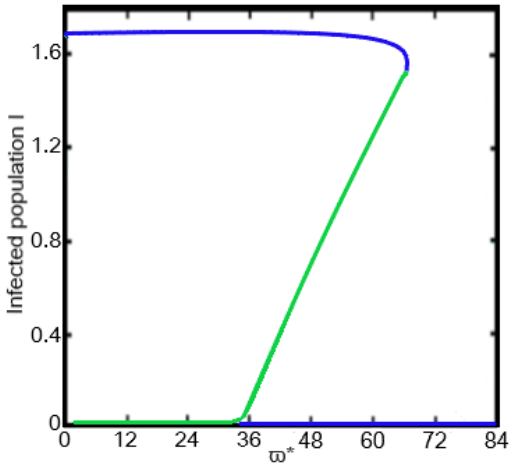


Figure 8: Bifurcation diagram for Marburg disease (2.1). The values of the parameter used here are taken from the Table 1 below. The bifurcation depicted here is of type backward bifurcation (involving the endemic equilibrium point (blue line) and the disease free equilibrium (green line)) and it indicates the well known classical epidemiological condition for the disease to die out ($\mathcal{R}_0 < 1$) is not sufficient anymore, but remains necessary.

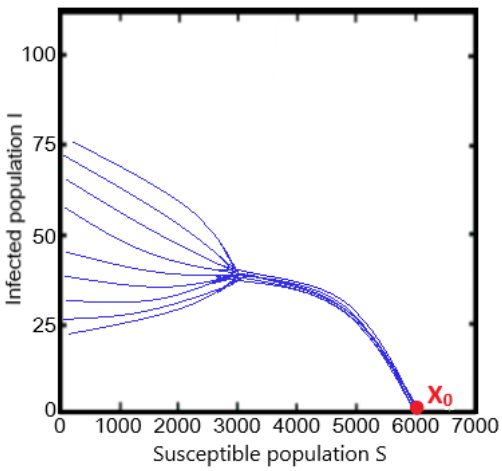


Figure 9: Possible existence of globally stability for the DFE $X_o$ of the model (2.1), with $\mathcal{R}_0<1$, $(0.3813)$ and $\beta=0.01$ and $k=0.2$.

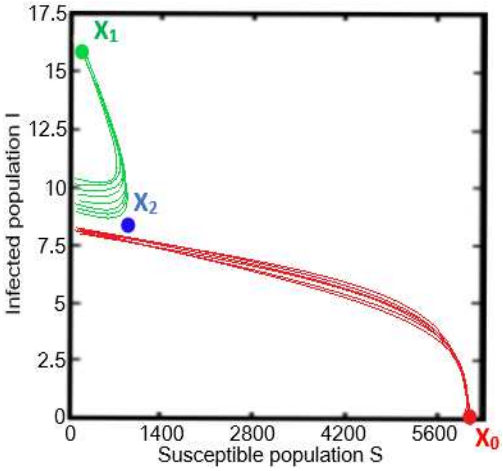


Figure 10: Possible existence of stability for two equilibria: The DFE $X_o$ and the endemic equilibrium $X_1$, and existence of instability for the endemic equilibrium $X_2$ of the model (2.1), with $\mathcal{R}_0<1,(0.7433)$ and $\beta=0.3$ and $k=0.4$.

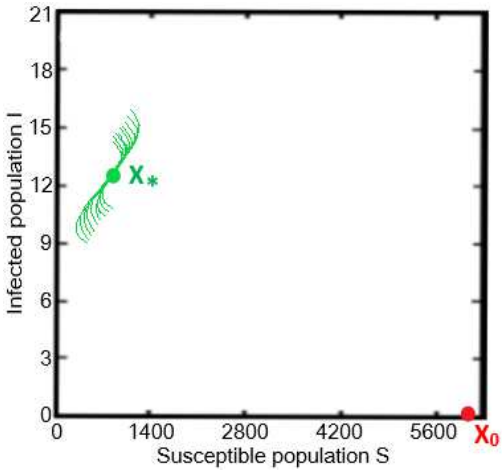


Figure 11: Possible existence of globally stability for the endemic equilibrium $X_*$ and instability for the DFE $X_o$ of the model (2.1), with $\mathcal{R}_0>1$, $(1.0074)$ and $\beta=1.3$ and $k=5\times10^{-2}$.

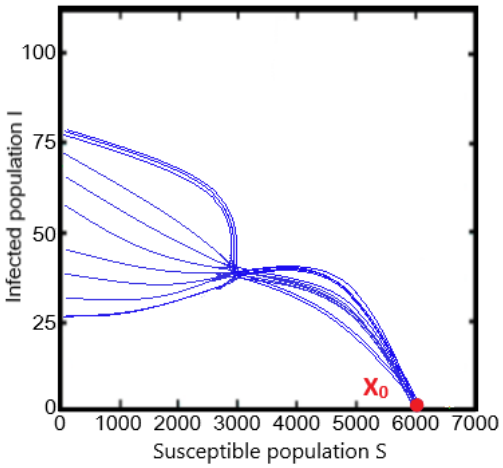


Figure 12: Possible existence of globally stability for the DFE $X_o$ of the model (4.1), with $\mathcal{R}_0<1$, $(0.3813)$ and $\beta=0.01$ and $k=0.2$.

spectively. It applies to the same equilibrium points but the trajectories are slightly different due the impact of the Mittag-Leffler kernel, which however, conserve the type of stability for the equilibria involved in the precess. The whole trajectories, convergent to the DFE $X_o=(6000,0,0,6000)$ in one case and convergent to the endemic equilibrium $X_*=(9.9,7.2,5.3,5748)$ in the other case are shown in Figs. 15-18 and they reflect the usual threshold behaviour.

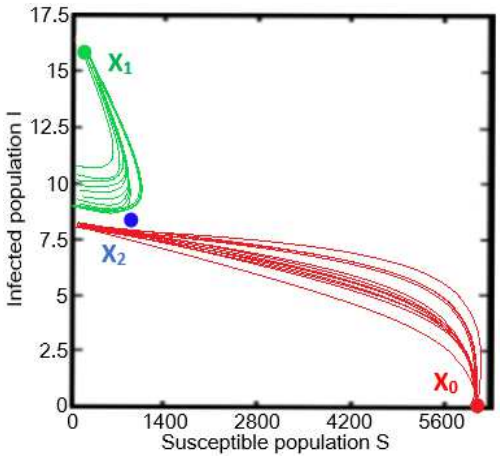


Figure 13: Possible existence of stability for two equilibria: The DFE $X_o$ and the endemic equilibrium $X_1$, and existence of instability for the endemic equilibrium $X_2$ of the model (4.1), with $\mathcal{R}_0<1,(0.7433)$ and $\beta=0.3$ and $k=0.4$.

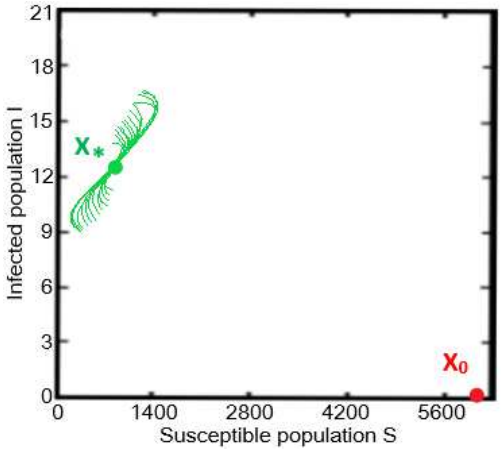


Figure 14: Possible existence of globally stability for the endemic equilibrium $X_*$ and instability for the DFE $X_o$ of the model (4.1), with $\mathcal{R}_0>1$, $(1.0074)$ and $\beta=1.3$ and $k=5\times10^{-2}$.

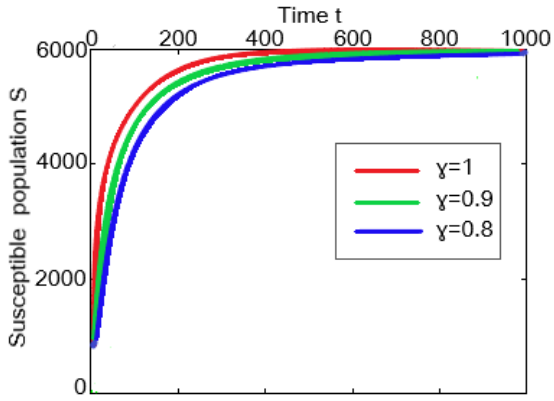


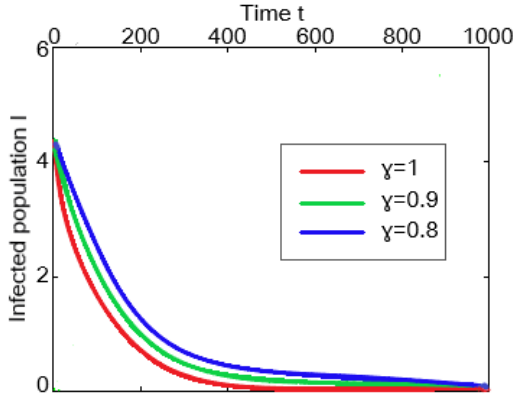


Figure 15: Dynamics of the model (4.1) showing the Marburg disease evolution using the Table 1 for three values of the parameter $\gamma$, which are $\gamma=0.8,0.9$ and 1. We observe similar trajectories reflecting the usual threshold behavior with a dynamic all converging to the DFE $X_o=(6000,0,0,6000)$.

As Ebola virus disease, the Marburg virus disease remains a constant threat to people's live, especially in the regions where previous outbreaks have been recorded or where the inhabitants share space with wild animals such as apes, monkeys and fruit bats on a daily basis. That is why it is important to know the real dynamics of the MVD very well in order to put in place suitable measures to tackle it when it outbreaks. This is also important in the search for adequate cure that can help save lives.

Affected areas and people living in should always be well informed about the nature of the disease. They should also be aware of the key public health recommendation notices given by scientists, experts and decision makers. Some of them include:

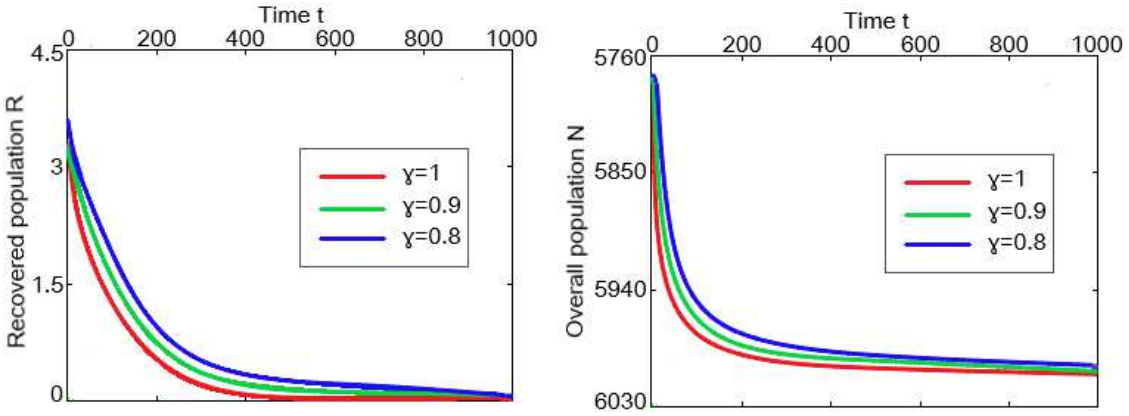


Figure 16: Dynamics of the model (4.1) showing the Marburg disease evolution using the Table 1 for three values of the parameter $\gamma$, which are $\gamma = 0.8, 0.9$ and 1. We observe similar trajectories reflecting the usual threshold behavior with a dynamic all converging to the DFE $X_o = (6000, 0, 0, 6000)$.

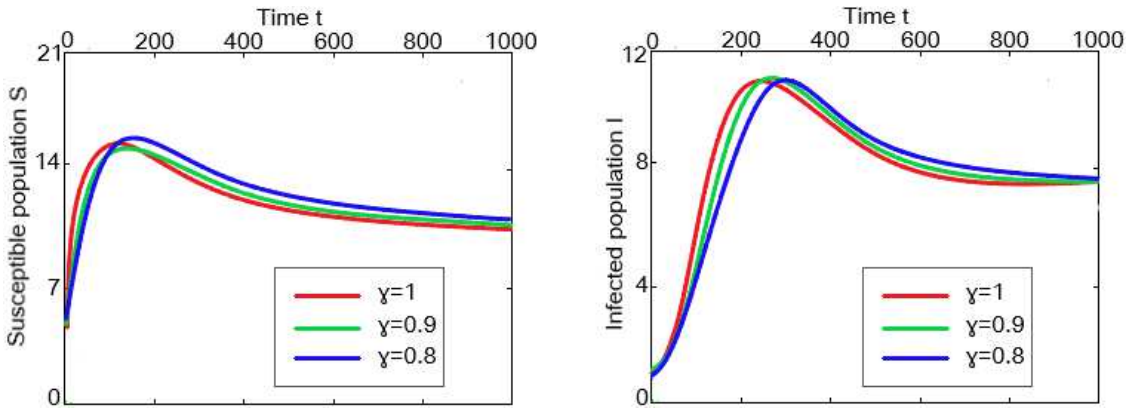


Figure 17: Dynamics of the model (4.1) showing the Marburg disease evolution using the Table 1 for three values of the parameter $\gamma$, which are $\gamma = 0.8, 0.9$ and 1. We observe similar trajectories reflecting the usual threshold behavior with a dynamic all converging to the endemic equilibrium $X_* = (9.9, 7.2, 5.3, 5748)$.

- Clear directions on how to quickly stop the spread of the Marburg virus in affected communities, especially the spread caused by contact with infected people in the community via bodily fluids. Such contacts should be avoided.
- Clear directions on how to quickly transfer, isolate and start treating any case suspected to be related to Marburg virus. Such isolation and treatment should be handled, not at home, but is an equipped health facility with qualified practitioners.
- Clear directions on how to behave when a suspected transfer happens, like using suitable personal protective equipment and regular hand washing.
- Clear directions on how to behave during burial ceremonies. People who have passed away due to Marburg disease should be quickly and safely buried without any direct contact with anyone.

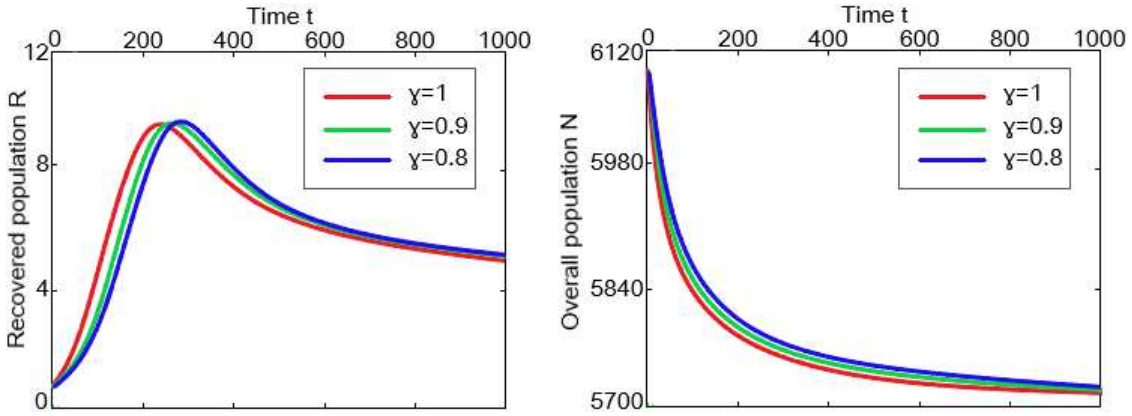


Figure 18: Dynamics of the model (4.1) showing the Marburg disease evolution using the Table 1 for three values of the parameter $\gamma$, which are $\gamma=0.8,0.9$ and 1. We observe similar trajectories reflecting the usual threshold behavior with a dynamic all converging to the endemic equilibrium $X_*=(9.9,7.2,5.3,5748)$.

- Clear directions on how to quickly stop the wildlife-to-human spread of the Marburg virus by adhering to regular hand hygiene when touching or handling any animal products related to apes, monkeys and fruit bats. Avoiding eating raw wild meat and the meat which has to be consumed should be well and thoroughly cooked.
- Lastly, clear directions on how to conduct visits or research in both the forests dominated by apes or monkeys and caverns or grottos inhabited by fruit bats. Personal protective outfits together with masks and gloves should always be worn during these visits.

## References

[1] M. S. Abdo, K. Shah, H. A. Wahash, and S. K. Panchal, *On a comprehensive model of the novel coronavirus (COVID-19) under Mittag-Leffler derivative*, Chaos Solit. Fractals, 135:109867, 2020.

[2] E. Ahmed, A. El-Sayed, and H. A. El-Saka, *On some Routh-Hurwitz conditions for fractional order differential equations and their applications in Lorenz, Rössler, Chua and Chen systems*, Phys. Lett. A, 358(1):1–4, 2006.

[3] I. Ahmed, E. F. Doungmo Goufo, A. Yusuf, P. Kumam, P. Chaipanya, and K. Nonlaopon, *An epidemic prediction from analysis of a combined HIV-COVID-19 co-infection model via ABC-fractional operator*, Alex. Eng. J., 60(3):2979–2995, 2021.

[4] Y. Araf, S. T. Maliha, J. Zhai, and C. Zheng, *Marburg virus outbreak in 2022: A public health concern*, The Lancet Microbe, 4(1):e9, 2023.

[5] S. Asawasamrit, A. Kijjathanakorn, S. K. Ntouyas, and J. Tariboon, *Nonlocal boundary value problems for Hilfer fractional differential equations*, Bull. Korean Math. Soc., 55(6):1639–1657, 2018.

[6] Y. Chen, F. Liu, Q. Yu, and T. Li, *Review of fractional epidemic models*, Appl. Math. Model., 97:281–307, 2021.

[7] E. F. Doungmo Goufo, *Mathematical analysis of peculiar behavior by chaotic, fractional and strange multiwing attractors*, Int. J. Bifurc. Chaos, 28(10):1850125, 2018.
[8] E. F. Doungmo Goufo, *The proto-Lorenz system in its chaotic fractional and fractal structure*, Int. J. Bifurc. Chaos, 30(12):2050180, 2020.
[9] E. F. Doungmo Goufo, *Construction and analysis of symmetric Sprott B multi-attractors with electric implementation*, Phys. Scr., 99(12):125219, 2024.
[10] E. F. Doungmo Goufo, *Mirroring and nonlinear perturbation of a circuit's system with multiple attractors*, Math. Model. Anal., 29(4):731–752, 2024.
[11] E. F. Doungmo Goufo, S. Kumar, and S. Mugisha, *Similarities in a fifth-order evolution equation with and with no singular kernel*, Chaos Solit. Fractals, 130:109467, 2020.
[12] H. Feldmann and H.-D. Klenk, *Filoviruses: Marburg and Ebola*, in: Advances In Virus Research, Vol. 47, Academic Press, 1–52, 1996.
[13] E. Fendzi-Donfack et al., *Nuclei discovered new practical insights via optimized soliton-like pulse analysis in a space fractional-time beta-derivatives equations*, Sci. Rep., 15(1):8440, 2025.
[14] E. Fendzi-Donfack and A. Kenfack-Jiotsa, *Extended Fan's sub-ODE technique and its application to a fractional nonlinear coupled network including multicomponents – LC blocks*, Chaos Solit. Fractals, 177:114266, 2023.
[15] T. Geisbert and P. Jahrling, *Differentiation of filoviruses by electron microscopy*, Virus Res., 39(2-3):129–150, 1995.
[16] P. Hovette, *Epidemic of Marburg hemorrhagic fever in Angola*, Médecine Tropicale: Revue du Corps de Sante Colonial, 65(2):127–128, 2005.
[17] B. Jeffs et al., *The médecins Sans Frontiéres intervention in the Marburg hemorrhagic fever epidemic, Uige, Angola, 2005. I. Lessons learned in the hospital*, J. Infect. Dis., 196(Supplement_2):S154–S161, 2007.
[18] A. Khan, T. Abdeljawad, M. Abdel-Aty, and D. K. Almutairi, *Digital analysis of discrete fractional order cancer model by artificial intelligence*, Alex. Eng. J., 118:115–124, 2025.
[19] A. Khan, T. Abdeljawad, and H. M. Alkhawar, *Digital analysis of discrete fractional order worms transmission in wireless sensor systems: Performance validation by artificial intelligence*, Model. Earth Syst. Environ., 11(1):25, 2025.
[20] M. A. Khan and A. Atangana, *Dynamics of ebola disease in the framework of different fractional derivatives*, Entropy, 21(3):303, 2019.
[21] M. A. Khan, S. Ullah, and M. Farooq, *A new fractional model for tuberculosis with relapse via Atangana-Baleanu derivative*, Chaos Solit. Fractals, 116:227–238, 2018.
[22] J. H. Kuhn et al., *New filovirus disease classification and nomenclature*, Nat. Rev. Microbiol., 17(5):261–263, 2019.
[23] S. Languon and O. Quaye, *Filovirus disease outbreaks: A chronological overview*, Virol.: Res. Treat., 10:1178122X19849927, 2019.
[24] W. Lin, *Global existence theory and chaos control of fractional differential equations*, J. Math. Anal. Appl., 332(1):709–726, 2007.
[25] F. Liu and F. Wei, *An epidemic model with Beddington-DeAngelis functional response and environmental fluctuations*, Phys. A, 597:127321, 2022.
[26] D. Matignon, *Stability results for fractional differential equations with applications to control processing*, in: Proceedings of the Computational Engineering in Systems and Applications, Vol. 2, IEEE, 963–968, 1996.
[27] N. Ndayimirije and M. K. Kindhauser, *Marburg hemorrhagic fever in Angola – Fighting fear and a lethal pathogen*, N. Engl. J. Med., 352(21):2155–2157, 2005.
[28] I. Petráš, *Fractional-Order Nonlinear Systems: Modeling, Analysis and Simulation*, in: Nonlinear

Physical Science, Springer Science & Business Media, 2011.
[29] S. Pooseh, H. S. Rodrigues, and D. F. Torres, *Fractional derivatives in dengue epidemics*, AIP Conf. Proc., 1389(1):739–742, 2011.
[30] R. Sampurna, *Pathology of Marburg virus disease (Marburg hemorrhagic fever)*, Infectious Disease Online, 2022. http://www.histopathology-india.net/marburg_virus.htm
[31] J. Schauder, *Der Fixpunktsatz in Funktionalraümen*, Studia Math., 2:171–180, 1930.
[32] K. Shifflett and A. Marzi, *Marburg virus pathogenesis – differences and similarities in humans and animal models*, Virol. J., 16(1):165, 2019.
[33] W. Slenczka and H. D. Klenk, *Forty years of Marburg virus*, J. Infect. Dis., 196(Supplement_2):S131–S135, 2007.
[34] M. Toufik and A. Atangana, *New numerical approximation of fractional derivative with non-local and non-singular kernel: Application to chaotic models*, Eur. Phys. J. Plus, 132(10):444, 2017.
[35] F. Wei and R. Xue, *Stability and extinction of SEIR epidemic models with generalized nonlinear incidence*, Math. Comput. Simulation, 170:1–15, 2020.
[36] World Health Organization, *Marburg virus disease – Guinea*, 2021. https://www.who.int/emergencies/disease-outbreak-news/item/2021-DON331
[37] World Health Organization, *Marburg virus disease – Uganda*, 2017. https://www.who.int/emergencies/disease-outbreak-news/item/25-october-2017-marburg-uganda-en
[38] World Health Organization, *DR Congo: WHO tracks deadly mysterious illness*, 2025. https://news.un.org/en/story/2025/02/1160596.